Asymmetrical surface soliton trains*

Yin Guo-Yan(尹国彦), Zheng Jiang-Bo(郑江波), Yang Xiao-Yu(杨晓雨), and Dong Liang-Wei(董亮伟)†

Institute of Information Optics, Zhejiang Normal University, Jinhua 321004, *China*

(Received 5 May 2009; revised manuscript received 31 July 2009)

We elucidate the existence, stability and propagation dynamics of multi-spot soliton packets in focusing saturable media. Such solitons are supported by an interface beside which two harmonically photonic lattices with different modulation depths are imprinted. We show that the surface model can support stable higher-order structures in the form of asymmetrical surface soliton trains, which is in sharp contrast to homogeneous media or uniform harmonic lattice modulations where stable asymmetrical multi-peaked solitons do not exist. Surface trains can be viewed as higher-order soliton states bound together by several different lowest order solitons with appropriate relative phases. Their existence as stable objects enriches the concept of compact manipulation of several different solitons as a single entity and offers additional freedom to control the shape of solitons by adjusting the modulation depths beside the interface.

Keywords: soliton trains, surface solitons, photonic lattices

PACC: 4265, 4225B, 4265S, 9210H

1. Introduction

Solitons in nonlinear systems play a crucial role in many branches of nonlinear science, such as biology, solid state physics, Bose–Einstein condensates, and nonlinear optics.[1] Lattice solitons are attracting intense attention these days due to the fact that optical lattice can provide an effectively tunable potential for guiding and controlling the dynamics of spatial solitons.[2,3] Various types of lattice solitons have been theoretically predicted and experimentally observed.[4−10]

The presence of interface separating nonlinear media with different optical properties substantially modifies the dynamics of solitons. Recently, self-trapped nonlinear surface states (surface solitons) have attracted a great deal of interest in abundant optical systems, including the prediction of one-dimensional (1D) surface gap solitons[11] and their observation.[12] It was demonstrated that 1D composite Bessel optical lattices with different lattice orders beside an interface can support stable surface solitons.[13] Theoretical studies of surface solitons in two-dimensional (2D) systems have been reported[14,15] and observed in experiment.[16,17] In particular, the existence and rigorous stability analysis of lattice solitons, in the form of soliton packets, in saturable media has been studied.[18] Surface soliton trains at the edge of a 2D photonic lattice have been observed.[19] Suitable periodic structures with engineered properties can be made in waveguide arrays with technologies currently available. Optical induction of the lattice is an effective alternative.[20] New types of interfaces can be produced by lattices with different symmetry or modulation parameters, opening new possibilities for exploring the properties of surface solitons.[21]

However, little attention has been paid to the dynamics of surface solitons supported by an interface separating two harmonically photonic lattices with different modulation depths, especially in photorefractive media with saturable nonlinearity. In this paper, we reveal that the surface model supports soliton trains that have no analogue in bulk uniform materials. The asymmetrical surface solitons are stable when their energy flow exceeds a certain threshold value. Intuitively, surface soliton trains can be built from an arbitrary number of different lowest order solitons, or soliton bits, with appropriately engineered phases. Our finding constitutes an example of a nontrivial soliton structure guided by an interface.

2. Model

We consider an optical beam propagation along the z-axis at an interface separating two harmonic lat-

*Project supported by the National Natural Science Foundation of China (Grant No. 10704067).

†Corresponding author. E-mail: donglw@zjnu.cn

© 2010 Chinese Physical Society and IOP Publishing Ltd

tices with different depths imprinted in focusing media with Kerr-type saturable nonlinearity. It can be described mathematically by the nonlinear Schrödinger equation for the dimensionless amplitude of a light field q

$$\mathrm{i}\,\frac{\partial q}{\partial z} = -\frac{1}{2}\frac{\partial^2 q}{\partial x^2} - \frac{|q|^2 q}{1+s|q|^2} - V(x)q, \qquad (1)$$

where the transverse x and the longitudinal z coordinates are scaled in terms of beam width and diffraction length respectively, s is a saturation parameter which weakens the focusing effect. The optical lattice is induced by the interference of a pair of plane waves which can be expressed as $V(x) = p_{\rm l}\cos(2\pi x/T)$ for $x \le 0$ and $V(x) = p_{\rm r}\cos(2\pi x/T)$ for $x > 0$, where $p_{\rm l,r}$ characterises the depth of refractive-index modulation on the left and right sides of the interface, and T is the modulation period. The depth of optical lattice is chosen to be comparable to the nonlinear contribution to the refractive index. Note that equation (1) admits several conserved quantities including the energy flow (power) U given by

$$U = \int_{-\infty}^{\infty} qq^* \mathrm{d}x. \qquad (2)$$

We stress that the above surface model is expected to hold for other systems, e.g., Bose–Einstein condensates with attractive interatomic interactions.

Two harmonic lattices with different depths beside the interface separating them can be fabricated technologically, e.g. by etching a waveguide array on a nonlinear substrate at $x > 0$ and another waveguide array with higher (lower) index at $x < 0$.[22] Optical induction offers a powerful alternative. To form the harmonically photonic lattice, a periodic pattern induced by two interfering plane waves is imprinted into a photorefractive crystal. The depth of the optical lattice can be adjusted by varying the intensity of the interfering plane wave. To realise the different modulation depths beside the interface, one can conveniently introduce an attenuating plate at $x < 0$ ($x > 0$) in front of the nonlinear crystal. Two optical lattices beside the interface can also be obtained by inputting two pairs of interfering plane waves along the same direction but with different frequencies. The redundant lattices on left and right sides of the interface can be removed by placing two filters with wavelengths corresponding to the inputting ones. The saturable nonlinearity is feasible in crystals whose photosensitivity strongly depends on wavelength.[11] Note that the lattice beam and the soliton beam should be launched in the ordinary and extraordinary polarisation directions of the crystal respectively.

3. Theoretical analysis

We search for soliton solutions of Eq. (1) in the form $q(x,z) = w(x)\exp(\mathrm{i}\,bz)$, where $w(x)$ is a real function describing the stationary solution profile of a soliton and b is a nonlinear propagation constant. Families of lattice solitons are determined by the propagation constant b, modulation period T, lattice depth $p_{\rm l,r}$ and saturation parameter s. Since the scaling transformation $q(x,z,s,p_{\rm r,l}) \to \chi q(\chi x, \chi^2 z, \chi^{-2}s, \chi^2 p_{\rm r,l})$ can be used to obtain various families of lattice solitons from a given one, we fix the modulation period $T = \pi/2$ and vary b, s, $p_{\rm r,l}$ throughout the paper without loss of generality. Stationary solutions of solitons can be obtained by solving Eq. (1) with a standard relaxation method. To elucidate their instability properties, we searched for perturbed solutions of Eq. (1) in the form $q = (w + u + \mathrm{i}\,v)\exp(\mathrm{i}\,bz)$, where $u(x)$ and $v(x)$ are real and imaginary parts of perturbation which can grow with a complex rate δ upon propagation. Substituting the perturbed solution into Eq. (1) and linearising it around w yields an eigenvalue problem

$$\delta u = -\frac{1}{2}\frac{\partial^2 v}{\partial x^2} + bv - Vv - \frac{w^2 + sw^4}{(1+sw^2)^2}v, \qquad (3)$$

$$\delta v = \frac{1}{2}\frac{\partial^2 u}{\partial x^2} - bu + Vu + \frac{3w^2 + sw^4}{(1+sw^2)^2}u. \qquad (4)$$

First, we discuss two types of fundamental surface solitons, on-site and off-site solitons [Figs. 1(a) and 1(b)]. The peaks of soliton profiles coincide with the peaks of the lattices. While the on-site soliton centres at the interface, the off-site soliton centres at the minimum of the lattice modulated deeper near the interface. Compared to the cases in non-surface lattices ($p_{\rm l} = p_{\rm r}$), surface solitons exhibit obvious asymmetry because of the different modulation depths beside the interface. For fixed $p_{\rm l,r}$, the energy flow is a monotonically increasing function of propagation constant for both on-site and off-site solitons [Fig. 1(c)]. Similar to the uniform media, the energy flow approaches infinity when $b \to b_{\rm upp}$. Unlike the uniform media, the energy flow does not approach zero.

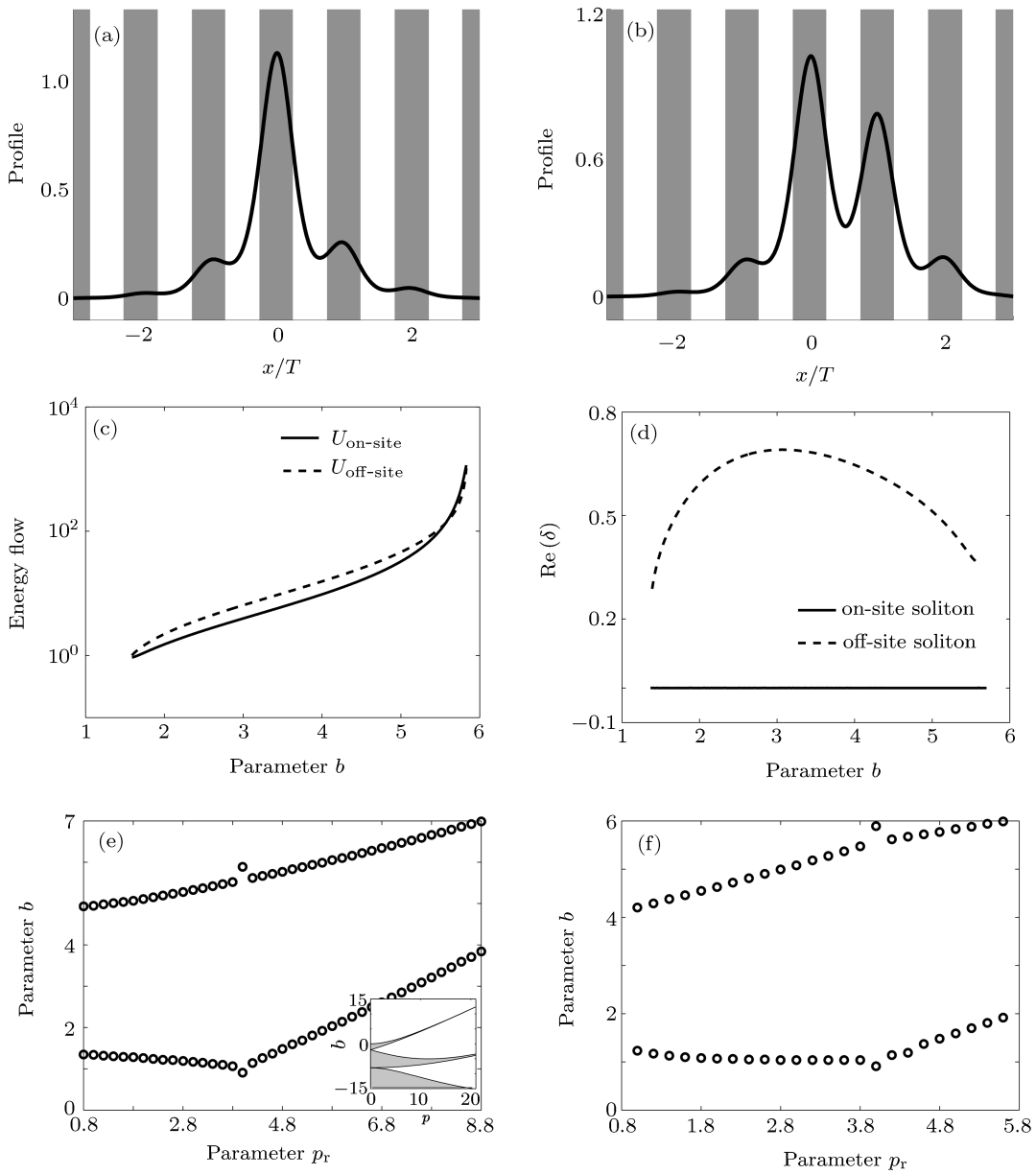


Fig. 1. Profiles of on-site (a) and off-site (b) surface solitons at $p_l = 4$, $p_r = 4.6$, $b = 1.5$. Grey regions correspond to $V(x) > 0$ and white regions correspond to $V(x) \leq 0$. (c) Energy flow versus propagation constant for on-site and off-site solitons at $p_l = 4$, $p_r = 5$. (d) Perturbation growth rate versus propagation constant for on-site and off-site surface solitons at $p_l = 4$, $p_r = 4.6$. Lower and upper cutoffs for the existence of on-site (e) and off-site (f) solitons versus p_r for $p_l = 4$. Saturation parameter $s = 0.2$. Inset in (e) depicts the band-gap structure of the periodic lattice, bands are shown in grey and gaps in white.

There exist lower (b_{low}) and upper (b_{upp}) cutoffs on propagation constant for both on-site and off-site solitons. The existence domains of on-site and off-site solitons are displayed in Figs. 1(e) and 1(f). For $p_l = 4$, with increasing modulation depth p_r, the lower cutoff b_{low} decreases slightly when $p_r < p_l$, and increases almost linearly when $p_r > p_l$. The maximum existence scope occurs when $p_l = p_r$ which corresponds to the non-surface case. The formation of upper cutoffs in terms of propagation constant is due to the saturable nonlinearity which can be seen as a weakened Kerr nonlinearity. The lower cutoffs associate with the hybrid band-gap structures of the optical lattices with different Floquet–Bloch spectra [inset in Fig. 1(e)]. All the solitons we have discussed reside in the common semi-infinity gap of the left and right lattices, which leads to the lower cutoffs being restricted by the upper edge of the first (hybrid) band. We also found unstable solutions for soliton residing in the first gap, which is not presented in this paper. Roughly speaking, the existence domain satisfies the relation $b_{\text{upp}} = b_{\text{low}} + 1/s$ if $p_l = p_r$. However, the presence of the interface and the hybrid band-gap structure destroys

the relationship. The existence domains of on-site and off-site solitons may broaden abruptly when $p_r = p_l$, which corresponds to the uniform harmonic modulation [Figs. 1(e) and 1(f)]. The existence areas shrink with the increase of parameter s for both on-site and off-site solitons. Linear stability analysis reveals that on-site surface solitons are completely stable in their existence domain but off-site solitons are always unstable [Fig. 1(d)].

Now we present families of twisted lattice solitons (soliton trains). Note that such solitons are usually also called out-of phase or staggered solitons. The amplitude of the soliton profile changes its sign between the neighbouring maxima of the lattice. Figures 2(a), 2(b) and 2(c) display some typical soliton profiles residing near the interface. The soliton solutions demonstrate strong asymmetry and can be intuitively viewed as nonlinear superposition of several different on-site solitons with appropriately engineered phases. The corresponding dispersion curve is a monotonically increasing function of propagation constant b [Fig. 2(d)].

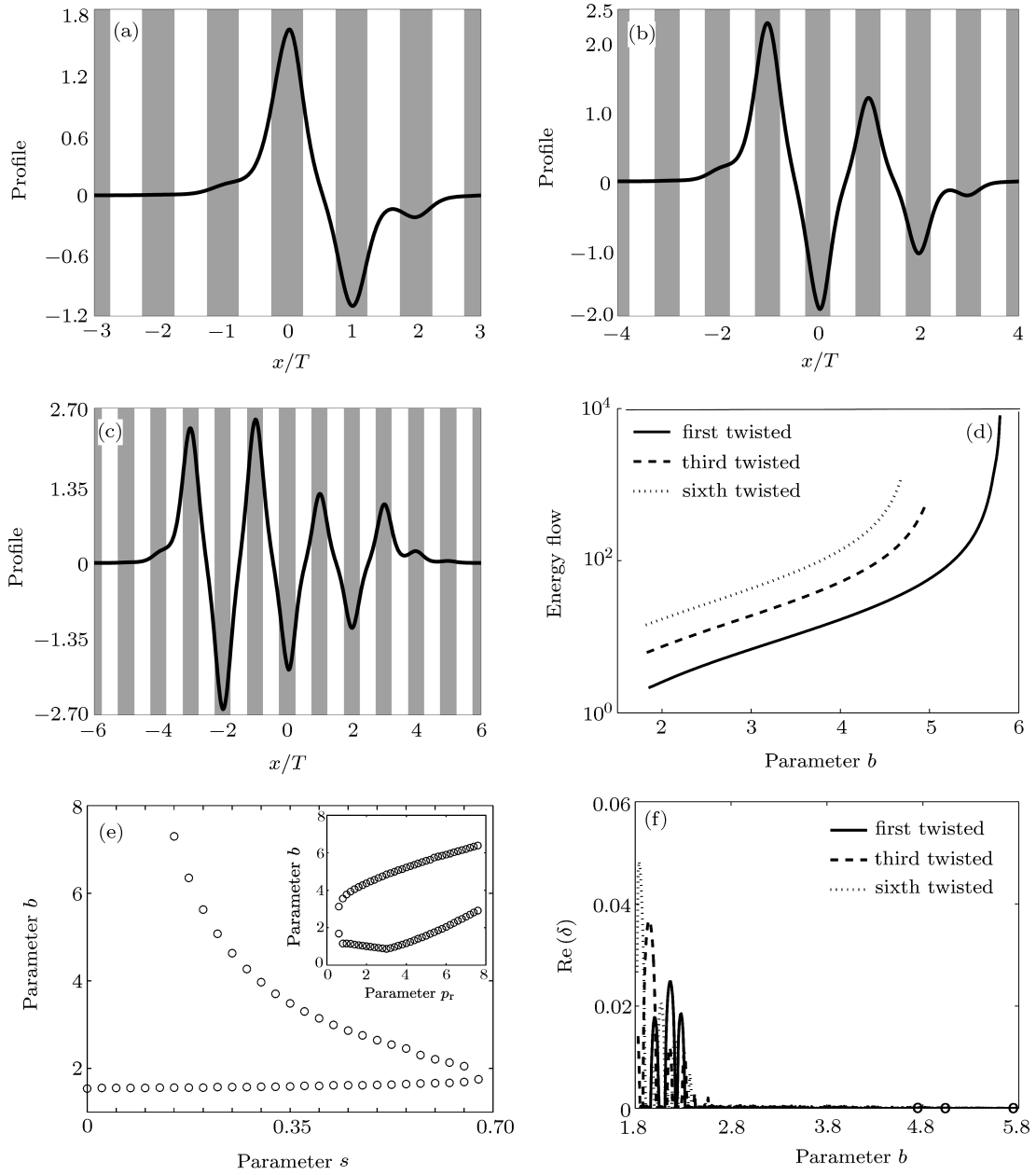


Fig. 2. Profiles of the first (a), third (b) and sixth (c) twisted solitons at $p_l = 3$, $p_r = 5.6$, $b = 3$. (d) Energy flow versus propagation constant for surface solitons displayed in (a)–(c). (e) Lower and upper cutoffs of the first twisted solitons versus saturation parameter s at $p_l = 3$, $p_r = 5$. Inset: lower and upper cutoffs of the first twisted solitons versus p_r for $p_l = 3$. (f) Instability growth rate versus propagation constant for the twisted solitons at $p_l = 3$, $p_r = 5.6$. Circles at the transverse axis denote the propagation constant cutoff of the twisted solitons. Saturation parameter $s = 0.2$ except for (e).

The energy flow increases with the growth of the order of twisted solitons. Contrary to intuition, the amplitude of the right part of the soliton is smaller than that of the left part associated with the shallow lattice. It can be explained in physics that the formation of the soliton is due to the balance of diffraction, focusing nonlinearity and lattice effect. For other fixed parameters, the higher the lattice depth is, the less the focusing nonlinearity is needed. When the energy of the soliton is large enough, a single lattice site cannot imprison the solution as a fundamental soliton. The energy will penetrate through the neighbouring lattice site which results in the higher-order soliton structure [Figs. 2(b) and 2(c)].

The existence area of the first twisted solitons versus the saturable parameter s is shown in Fig. 2(e). It shrinks with the rise in s and disappears if $s > 0.65$. Similar to the cases of on-site solitons, the lower cutoff $b_{\rm low}$ decreases with $p_{\rm r}$ for $p_{\rm r} < p_{\rm l}$ and increases for $p_{\rm r} > p_{\rm l}$ for the first twisted soliton trains [inset plot in Fig. 2(e)]. Linear stability analysis indicates that soliton trains become stable when the propagation constant exceeds a certain threshold value [Fig. 2(f)]. In other words, the soliton train will be stable if its energy flow is high enough. The existence domains of the first, third and sixth soliton trains are $b \in [1.85,\ 5.79], [1.85,\ 4.98]$ and $[1.85,\ 4.69]$ respectively. The stability windows are about $88\%, 84\%$ and 81% of their existence windows. One can expect that soliton trains including more components also exist and are stable in a relatively wide parameter window. The structure of instability area is rather complicated. Stable twisted solitons with propagation constant in some separated stability windows are also possible, as illustrated in Fig. 2(f). There exist very narrow instability bands near the upper cutoff curve and we do not discuss it since the corresponding energy flow approaches infinity.

The central result of this paper is that the interface model can support a stable soliton train which can contain an arbitrary number of components when its energy flow exceeds a certain threshold value. The higher-order soliton structure can be viewed as nonlinear superposition of several different on-site solitons with opposite phases and can be built by several different individual on-site solitons. The threshold energy flow (propagation constant) for stabilisation of surface solitons slowly increases with growth of soliton order, i.e., the number of spots in the soliton packet [Fig. 2(f)]. Physically, stabilisation of the soliton trains can be understood as follows. Since the alternating phases of the neighbouring lowest-order spots are involved in the packets, the interaction forces between them are repulsive. While higher-order soliton complexes cannot exist as stable objects in uniform media, the effective potential induced by the lattices compensates such repulsive forces and results in stable propagation.

4. Numerical simulations

To confirm the results of the linear stability analysis, we exhaustively simulate Eq. (1) with the input condition as $q(x, z = 0) = w(x)[1 + \rho(x)]$, where $\rho(x)$ is a random function with Gaussian distribution whose variance $\sigma^2_{\rm noise} = 0.01$. Figure 3 shows the stable propagation of perturbed surface solitons displayed in Figs. 1(a), 2(a), 2(b), and 2(c). The asymmetrical surface solitons immediately radiate away the initially added noises and their soliton shapes remain after propagating a short distance, which exceeds the experimentally feasible crystal length by about several orders.

The twisted solitons will break into single soliton components if we remove the lattice. The unpacking effects can be used to control the flying direction of soliton "bits". The escape angle of the unpacked solitons increases with the rise in lattice depth [Fig. 4(a) and 4(b)]. When b and $p_{\rm l}$, $p_{\rm r}$ are fixed simultaneously; the higher the number of solitons in the train is, the faster the train splits [comparing Fig. 4(c) with 4(d)]. The soliton "bits" experience complicated inelastic collisions immediately after the lattice is removed. Note that the main energy of the original twisted soliton converges to the outside soliton components by the energy coupling. Thus, the splitting process produces sets of soliton "bits" with controllable escape angles by varying the depths of the lattice on the two sides of the interface. The number of unpacked soliton components equals the number of peaks in soliton trains.

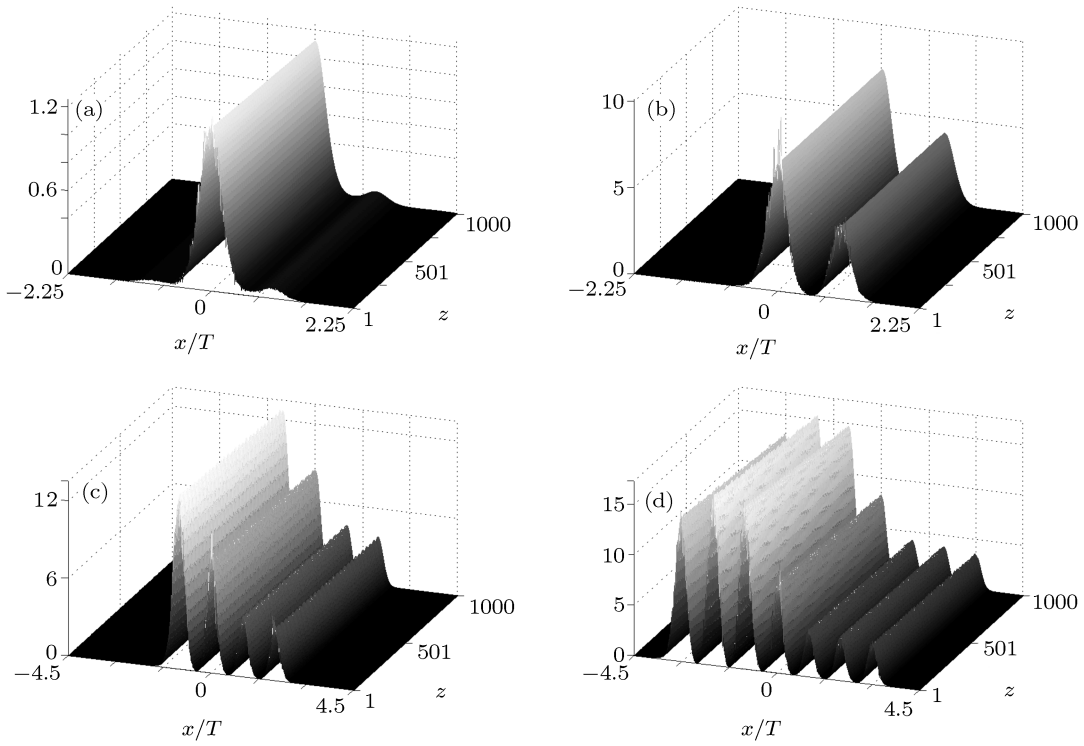


Fig. 3. Stable propagation of the simplest on-site surface soliton at $p_{\rm l} = 4$, $p_{\rm r} = 4.6$, $b = 1.5$ (a) and first (b), third (c), sixth (d) twisted solitons at $p_{\rm l} = 3$, $p_{\rm r} = 5.6$, $b = 3$. White noises with variance $\sigma^2_{\rm noise} = 0.01$ have been added into the initial input beams. Saturation parameter $s = 0.2$.

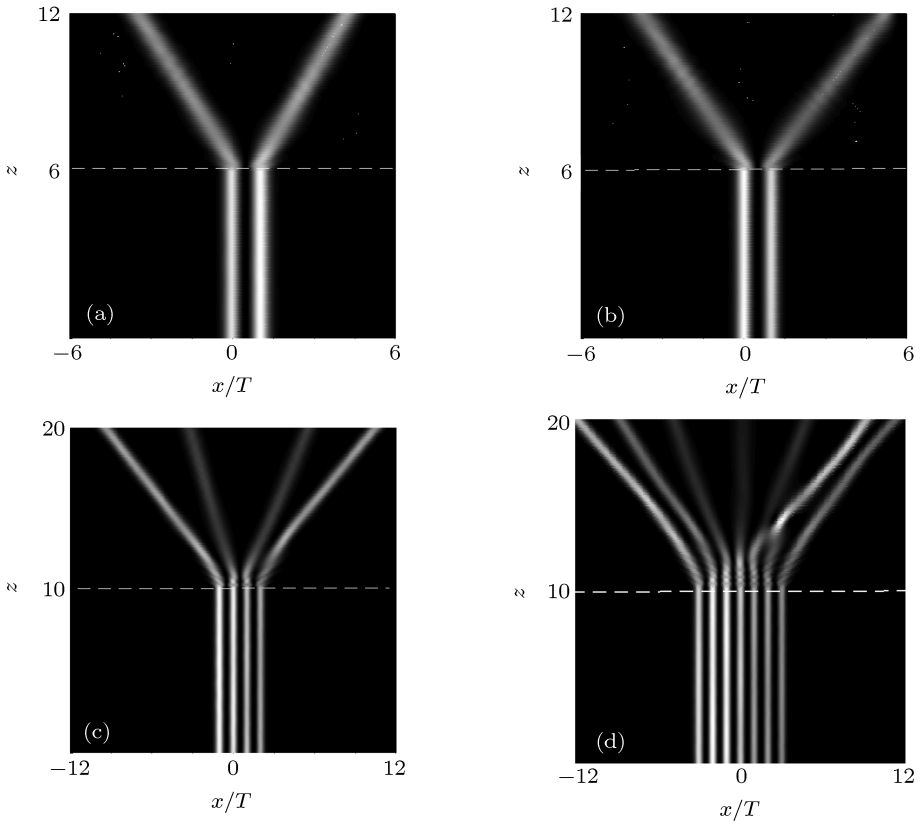


Fig. 4. Unpacking of the first twisted solitons at the boundary (dashed line) between uniform medium and lattice modulated medium at $p_{\rm r} = 2$ in (a) and $p_{\rm r} = 4$ in (b). Unpacking of the third (c) and sixth (d) twisted solitons. Saturation parameter $s = 0.2$. $p_{\rm l} = 3$, $b = 3$ in (a) and (b) and $p_{\rm l} = 3$, $p_{\rm r} = 4$, $b = 3$ in (c) and (d).

5. Discussions and conclusions

Our analysis is based on the different lattice depths beside the interface. The surface solitons will exhibit some novel properties if we vary the lattice depth and modulation period synchronously. For example, the interval of the peaks of soliton profiles will no longer be the same. Complicated analysis should be performed since the band-gap structure (related to the existence domain of solitons) will be very different. Our findings can also be generalised into $(2+1)$D schemes in which multi-ring necklace-like solitons and their unpacking phenomena may be observed.

In conclusion, we have studied the properties of surface lattice solitons supported by two photonic lattices with different modulation depths. We revealed that besides the simplest stable on-site solitons, the interface model also supports stably twisted solitons just like a "train". The twisted solitons demonstrate distinct asymmetry. They can be unpacked into several individual solitons flying away with certain escaping angles by removing the lattices. Such multi-spot soliton states can be viewed as a nonlinear superposition of several lowest order solitons bound together. Our research may open the possibility of the compact manipulation of many different solitons as a single state and can also be generalised to the case of Bose–Einstein condensates trapped in optical lattices with attractive interatomic interactions.

References

[1] Kivshar Yu S and Agrawal G P *Optical Solitons: from Fibres to Photonic Crystals* 2003 (San Diego: Academic)

[2] Fleischer J W, Segev M, Efremidis N K and Christodoulides D N 2003 *Nature* (London) **422** 147

[3] Rotschild C, Segev M, Xu Z, Kartashov Y V and Torner L 2006 *Opt. Lett.* **31** 3312

[4] Christodoulides D N, Lederer F and Silberberg Y 2003 *Nature* (London) **424** 817

[5] Martin H, Eugenieva E D, Chen Z G and Christodoulides D N 2004 *Phys. Rev. Lett.* **92** 123902

[6] Chen Z G, Martin H, Eugenieva E D, Xu J J and Bezryadina A 2004 *Phys. Rev. Lett.* **92** 143902

[7] Chen F, Stepić M, Rüter C, Runde D, Kip D, Shandarov V, Manela O and Segev M 2005 *Opt. Express* **13** 4314

[8] Lou C B, Wang X S , Xu J J, Chen Z G and Yang J K 2007 *Phys. Rev. Lett.* **98** 213903

[9] Wang X S, Chen Z G, Wang J D and Yang J K 2007 *Phys. Rev. Lett.* **99** 243901

[10] Hu Y, Lou C B, Liu S, Zhang P, Zhao J L, Xu J J and Chen Z G 2009 *Opt. Lett.* **34** 1114

[11] Kartashov Y V, Vysloukh V A and Torner L 2006 *Phys. Rev. Lett.* **96** 073901

[12] Rosberg C, Neshev D N, Krolikowski W, Mitchell A, Vicencio R A, Molina M I and Kivshar Yu S 2006 *Phys. Rev. Lett.* **97** 083901

[13] Dong L, Yang X and Chen H 2008 *Chin. Phys.* B **17** 988

[14] Makris K G, Hudock J, Christodoulides D N, Stegeman G I, Manela O and Segev M 2006 *Opt. Lett.* **31** 2774

[15] Kartashov Y V, Torner L and Vysloukh V A 2006 *Opt. Lett.* **31** 2595

[16] Wang X S, Bezryadina A, Chen Z G, Makris K G, Christodoulides D N and Stegeman G I 2007 *Phys. Rev. Lett.* **98** 123903

[17] Szameit A, Kartashov Y V, Dreisow F, Pertsch T, Nolte S, Tünnermann A and Torner L 2007 *Phys. Rev. Lett.* **98** 173903

[18] Kartashov Y V, Vysloukh V A and Torner L 2004 *Opt. Express* **12** 2831

[19] Wang X S, Samodurov A and Chen Z G 2008 *Opt. Lett.* **33** 1240

[20] Kartashov Y V and Torner L 2006 *Opt. Lett.* **31** 2172

[21] Ye F, Dong L and Hu B 2009 *Opt. Lett.* **34** 584

[22] Mandelik D, Eisenberg H S, Silberberg Y, Morandotti R and Aitchison J S 2003 *Phys. Rev. Lett.* **90** 053902